

Unexpected change in the electronic properties of the Au-graphene interface caused by tolueneH. Pinto,^{1,*} R. Jones,¹ J. P. Goss,² and P. R. Briddon²¹*School of Engineering, Mathematics and Physical Sciences, University of Exeter, Stocker Road, Exeter EX4 4QL, United Kingdom*²*School of Electrical, Electronic and Computer Engineering, Newcastle University, Newcastle Upon Tyne, England NE1 7RU, United Kingdom*

(Received 8 March 2010; revised manuscript received 21 May 2010; published 3 September 2010)

Density-functional theory is used to show that isolated Au atoms on graphene do not lead to substantial charge transfer or doping but this is altered if a second layer of graphene or toluene is present. Thus intercalating Au into a sandwich of graphene-toluene leads to *n*-type doping of graphene. The effect is attributed to a confinement of the 6*s* level of Au by toluene or the second graphene layer. It is also shown that K atoms dope graphene with the transfer of around one electron. The binding energies and electronic structure of Au, Cr, and Ti on graphene are also reported.

DOI: [10.1103/PhysRevB.82.125407](https://doi.org/10.1103/PhysRevB.82.125407)

PACS number(s): 73.22.Pr, 68.43.Bc, 73.20.Hb, 73.22.-f

I. INTRODUCTION

Graphene is a zero-gap semiconductor consisting of a monolayer of carbon atoms arranged in a two-dimensional honeycomb lattice.¹ The high mobility of its charge carriers combined with the effect of different dopants makes graphene a possible material for electronic applications.² The fabrication of electronic devices requires metal contacts, usually made of Ti, Cr, and Au, and thus understanding the properties of metallic adsorbates is of great importance. Electronic applications also require the control of the type and concentration of charge carriers which can be achieved by the deposition of atoms and molecules on the graphene surface.

Different adsorbates, either atoms or molecules, has been extensively studied both theoretically and experimentally. Previous density-functional calculations reported the geometry, binding energy, and electronic structure of different metals on graphene.³⁻⁷ For most of the metals studied, the preferred location on the graphene layer is the (H) site, directly above the center of the graphene hexagon. For Au, Ni, and Sn, however, the most stable site lies directly above a graphene carbon atom, (T) site while Pt and Cr atoms were found to be more stable above the C-C bond, (B) site. However, the migration energy of the metal across the surface of graphene is often low and the metal atom will easily diffuse and become trapped by other metal atoms or other adsorbates. For Ti, a migration barrier of 0.7 eV has been calculated while Pt and Au are highly mobile with barriers lower than 0.1 eV.³ If the diffusivity is given by $\sim a^2 \nu \exp(-W/kT)$, then the atoms will diffuse a distance of about 5 nm after one hour at room temperature.

Here we study the properties of a single metallic atom which is either bound to graphene or lies between graphene and a toluene overlayer. We use the local-density approximation (LDA) rather than the generalized gradient approximation (GGA) (Refs. 4-7) and this is necessitated as GGA underestimates interlayer binding energies causing graphite to be unstable. In addition, the binding energies of toluene and other hydrocarbons adsorbed on graphene are much lower than experimental values.⁸

Experimentally, Ti, Fe, and Pt transition-metal clusters have been deposited on graphene by molecular-beam

epitaxy.⁹ The doping properties of the adsorbates were explored in gated devices using *in situ* transport measurements (conductivity as function of gate voltage). For all the metal clusters investigated doped the graphene *n*-type and Ti was found to be the most effective donor. Depending on coverage, Pt can lead to either *n*-type or *p*-type doping. Theoretical calculations have also predicted Ti (Ref. 5) and K (Refs. 4 and 5) to be donors. Electron doping of graphene was also demonstrated with K atoms deposited at low temperatures (20 K) on graphene in ultrahigh vacuum.¹⁰ Whereas one expects that electropositive adsorbates will dope graphene *n*-type, molecular dopants could lead to either *n*-type or *p*-type doping. Thus, when exposed to CO and NH₃, graphene is doped *n*-type.¹¹ The opposite effect can be achieved with H₂O, NO₂, N₂O₄,^{11,12} and F4-TCNQ (tetrafluoro-tetracyanoquinodimethane) molecules.^{13,14} It should be remarked, however, that the mobility of carriers is expected to be reduced by the additional Coulomb scattering caused by the dopants. However, in some cases, e.g., NH₃, this does not occur and the mobility increases.¹¹ We shall discuss this in another paper. Another complexity can arise if two types of adsorbates are present neither of which has a doping effect on its own but when in combination, a doping effect is found. We shall show here that this is the case for toluene and gold on single layer graphene.

II. METHOD

Spin-optimized calculations were performed using the AIMPRO density-functional code.^{15,16} The LDA was used to represent the exchange correlation potential. The core electrons of the atoms were treated using the Hartwigsen Goedecker Hutter pseudopotentials.¹⁷ The spin populations of the cell were optimized by starting from random spin distributions. The orbitals of the valence electrons consist of independent *s*-, *p*-, *d*-like Gaussian functions centered on atoms.¹⁸ The electronic levels were filled using Fermi-Dirac statistics with $k_B T = 0.01$ eV and metallic filling. The system was modeled using a $4 \times 4 \times 1$ unit cell of graphene, enclosing 32 carbon atoms, with periodic boundary conditions. The Brillouin zone was sampled with a grid of $8 \times 8 \times 1$ **k** points within the Monkhorst-Pack scheme.¹⁹ Charge densities were

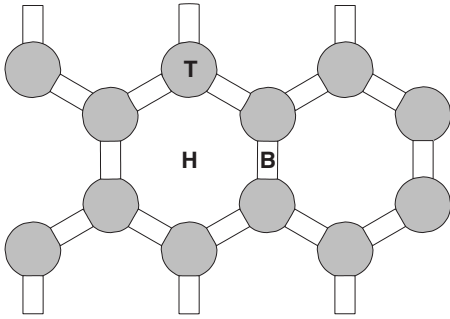


FIG. 1. Adsorption sites considered. T is directly on top of a carbon atom of graphene, H lies above the center of the hexagonal ring of carbon atoms in graphene, and B above a graphene C-C bond.

Fourier transformed using plane waves with an energy cutoff of 200 Ha.

The adsorption of single K, Au, Cr, and Ti atoms was studied in the three obvious adsorption graphene sites: above the center of the graphene hexagonal ring (H), above a C-C bond (B) and above the carbon atom (T), Fig. 1. A molecule of toluene was placed on top of a single adsorbed metal atom, itself on top of graphene, to investigate the effect of an overlayer of toluene on the electronic properties of metals deposited on graphene.

III. RESULTS

A. Toluene on graphene

Figure 2 shows the optimized bond lengths and angles of the isolated toluene molecule. The results are in good agreement with x-ray diffraction measurements shown in Table I.²⁰

The toluene molecule was placed above the graphene layer, in two different configurations, corresponding with AA

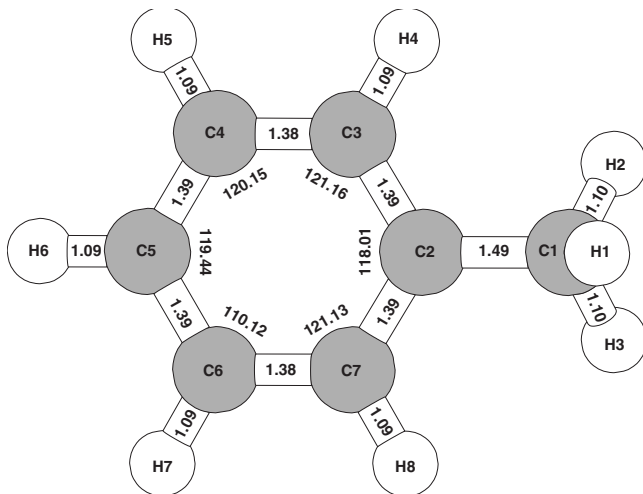


FIG. 2. Calculated molecular structure of toluene molecule. The molecule consists of a benzene ring in which one H atom is replaced by CH₃. The bond distances are given in angstroms and the angles in degrees.

TABLE I. Comparison between the calculated and the experimental (Ref. 20) bond lengths and bond angles of toluene molecule.

Bond	Calculated (Å)	Experimental (Å)
C1-C2	1.49	1.49
C2-C3	1.39	1.39
C3-C6	1.38	1.38
C6-C7	1.39	1.37
C3-H4	1.09	1.0
Angle		
C3-C2-C7	118.01	117.79
C4-C3-C2	121.16	121.03
C5-C4-C3	120.15	120.34
C6-C5-C4	119.44	119.47

and AB Bernal stacking. The minimum separation between the toluene molecules in different unit cells is 4.3 Å. Upon relaxation, we found the AB stacking configuration was more stable by 0.08 eV with the toluene molecule 3.2 Å above the graphene surface. There was no tendency, for the toluene coverage used, for the molecular plane to tilt with respect to the graphene plane. Figure 3 shows the relaxed structure. The binding energy between the molecule and graphene was found by finding the energy of the same sized cell when the distance between the molecule and graphene was increased to 8.5 Å. This energy is 0.6 eV and is comparable with the binding energy of benzene to graphene which was determined experimentally to be 0.5 eV.²¹

Figures 4(a) and 4(b) show the electronic band structure of pristine graphene and toluene on top of graphene. The adsorption of toluene does not perturb the electronic properties of graphene in the neighborhood of the Dirac point. In particular, the Fermi level remains at the Dirac point indicating the absence of charge transfer between the toluene and the graphene. This is entirely in agreement with expectation.

B. Isolated metals on graphene

We now consider the effect of individual metallic atoms on the electronic structure. The structure and binding energy for various metal atoms on graphene are shown in Table II. The most stable position for a Au atom is directly above a

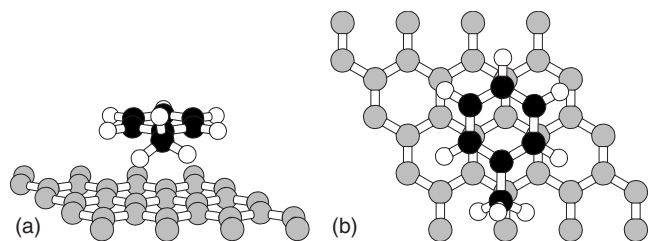


FIG. 3. (a) Side and (b) top view of the minimum energy configuration of the toluene molecule on top of the graphene surface.

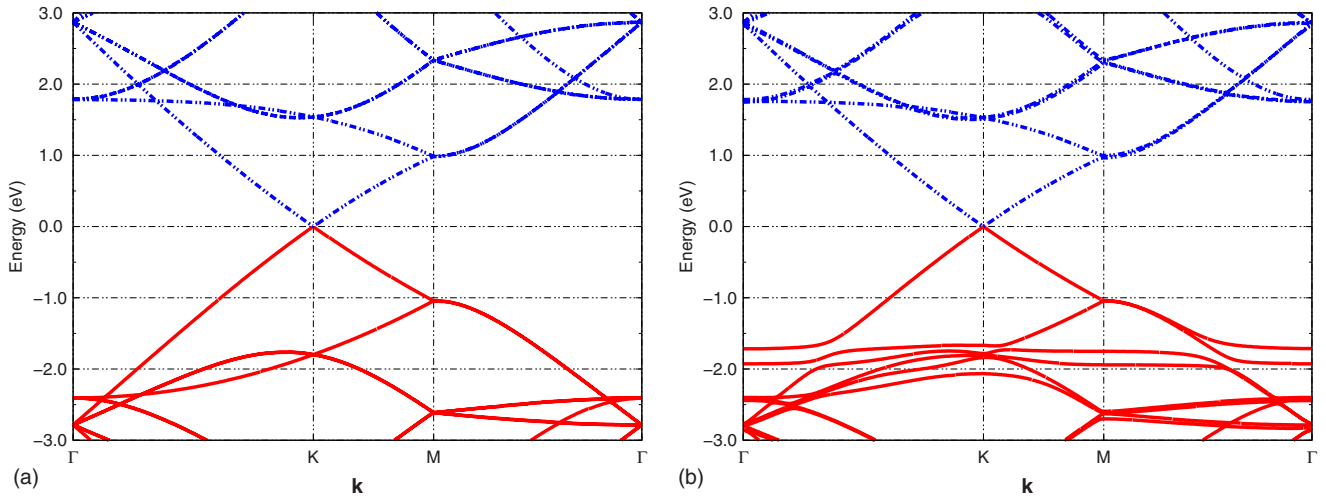


FIG. 4. (Color online) Band structure (eV) of (a) pristine graphene and (b) toluene molecule on top of graphene, plotted in the vicinity of the Fermi energy along the high-symmetry directions of the Brillouin zone. Full lines denote occupied states while dashed lines show empty levels. The Fermi level is placed at zero. Note that the electronic structure of graphene in this energy range is unaffected by toluene.

carbon atom, at a T site. All other metallic atoms prefer to lie above the middle of the hexagonal H site, hence maximizing the number of metal-carbon bonds. The geometric structure and binding energies are in good agreement with previous LDA calculations.³

Spin optimization of K above graphene shows that the ground state is a singlet. Figure 5 shows the spin-averaged electronic band structure for a K atom adsorbed on graphene.

In Fig. 5, the Fermi level lies above the Dirac point indicating substantial charge transfer from the K atom to the graphene. Integrating the density of states of pristine graphene to the Fermi level found for the metal on top of graphene, shows approximately one electron is transferred. Inspection of the wave function of the empty level marked A at the K point in Fig. 5, and shown in Fig. 6(a), demonstrates that the wave function is strongly localized on the K atom and originates from its spin-up $4s$ orbital which was occupied in the isolated atom. The wave function of the occupied level at the K point [the upper of the two levels marked B in Fig. 5] is shown in Fig. 6(b). It is delocalized over graphene and avoids the K atom. This level would have been unoccupied in graphene when the metal atom is not present. These results confirm that charge transfer has occurred from the $4s$ occupied level of K to graphene. This result is in agreement with previous experimental and theoretical work which dem-

onstrate K atoms act as donors on graphene.^{4,5,10}

Spin optimization of Au on graphene resulted in a magnetic moment of $1.0 \mu_B$. Figures 7(a) and 7(b) show the majority- and minority-spin electronic band structures of Au on graphene. Far from the K point, the flat band at Γ near to the Fermi level is strongly localized on the Au atom as shown in Fig. 8(a). When this $6s$ -Au level crosses the π and π^* bands, the bands hybridize and at the K point, the highest occupied level, marked B in Fig. 7(a), is delocalized over the graphene layer as shown in Fig. 8(b). Thus the occupancy of this band is unchanged from that of graphene. The level below the highest occupied level at the K point, marked C in Fig. 7(a), is localized on the Au atom, Fig. 8(c). Thus although the presence of a Au atom changes the band structure close to the Dirac point, there is no evidence of any significant charge transfer between Au and the graphene surface.

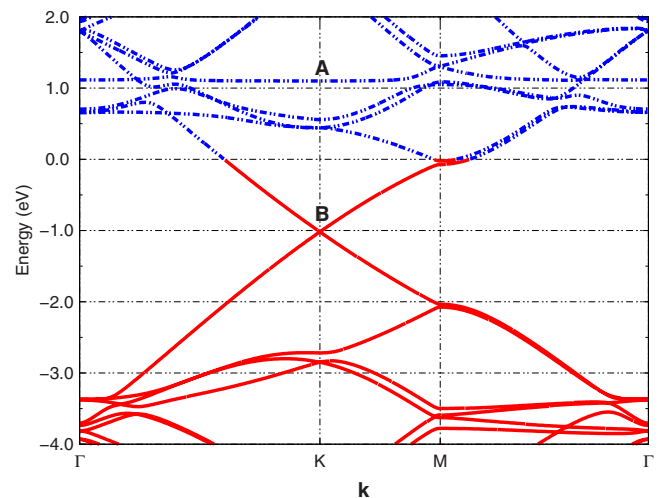


FIG. 5. (Color online) Spin-averaged electronic band structure (eV) of K on top of graphene in the vicinity of the Fermi energy. The Fermi level is set to zero. Full lines denote occupied states while dashed lines show empty levels. The bands around B, unoccupied for pristine graphene, are now occupied.

TABLE II. Metal-carbon bond lengths (\AA), perpendicular distances from the metal do the graphene layer plane (\AA), metal binding energies (eV), and magnetic moment (μ_B).

Metals	Eq. position	Bond length (\AA)	Height (\AA)	Binding energy (eV)	Magnetic moment (μ_B)
Au	T	2.27	2.27	0.65	1.0
K	H	2.82	2.42	1.51	0.0
Cr	H	2.43	1.99	0.88	5.0
Ti	H	2.27	1.75	2.55	3.1

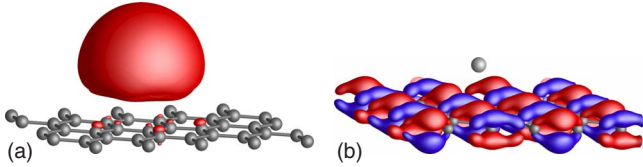


FIG. 6. (Color online) Plot of the real part of the wave functions of the electronic levels of a K atom on top of graphene at points marked (a) A and (b) B in Fig. 5. The wave function of the level marked A is localized on the K atom while the wave function of the highest occupied level, marked B, is delocalized over the graphene layer.

Au however is clearly a marginal case as if the 6s level was higher in energy, then charge transfer would occur. This result is in agreement with earlier calculations on bulk metals deposited on graphene.²²

The same analysis was used to study the effect of the adsorption of single Ti and Cr atoms on the electronic properties of graphene. We allowed the spin populations to adjust when the total energy is minimized. This leads to a magnetic moment for Ti and Cr of 3 μ_B and 5 μ_B , respectively. As shown in Fig. 9, the majority-spin Fermi levels of both metals lie above the Dirac point indicating that transfer of charge from the metal to graphene occurs making graphene *n*-type. This result agrees with recent experiments.⁹

C. Metals intercalated between toluene and graphene

The adsorption of metals intercalated with an overlayer of toluene and the graphene surface was also considered. The minimum energy sites for Ti, Cr, and K were found to be in the middle of the hexagonal ring of toluene and above a carbon atom of graphene, Fig. 10, while a Au atom lies beneath a carbon atom of the toluene ring and above a carbon atom of graphene. For K, Cr, and Au, the toluene molecule now is no longer parallel to the graphene layer but tilts with

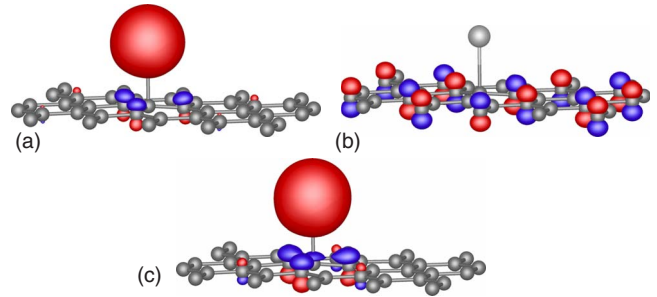


FIG. 8. (Color online) Plot of the real parts of the wave functions of the majority spin levels, marked A, B, and C in Fig. 8(c), for Au on top of graphene.

the methyl group pointing slightly to the graphene plane.

There are two binding energies to be considered. The toluene can be pulled away leaving the metal atom on top of graphene or the graphene pulled away leaving the metal atom bound to toluene. We refer to these as the energies required to break the toluene-metal bond and the graphene-metal bond and they are given in Table III.

The results suggest that the electropositive metals such as K are more strongly bound to graphene than toluene probably because of the electron transfer described above. Cr and Ti, which are carbide forming elements, are strongly bound to both toluene and graphene while Au, the least electropositive metal, is bounded weakly to toluene and graphene.

We then investigated the effect on the electronic structure of the metal bound to graphene caused by toluene and in the case of Au, we found that an unexpected doping now takes place. Spin optimization led, in contrast to the case of Au on graphene, to the transfer of spin-up electrons in state *k* to spin-down electrons in a different *k* state with a lower energy. Thus, like the case of K, the ground state is a spin singlet. The spin-averaged band structure of Au intercalated between toluene and graphene is shown in Fig. 11. The Fermi level of the former now lies above the Dirac point and

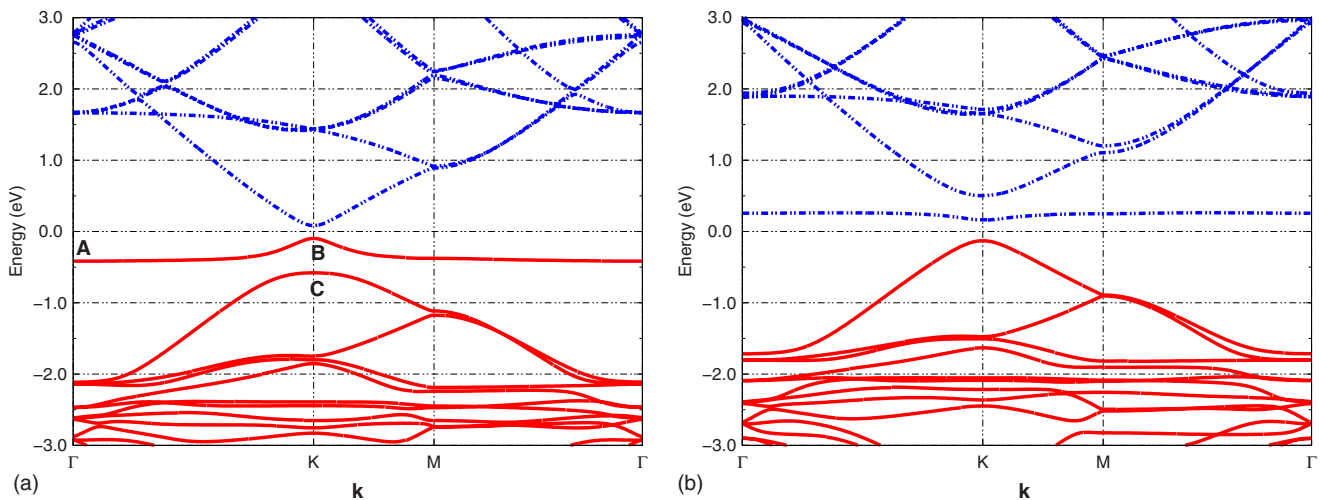


FIG. 7. (Color online) Spin-polarized band structures (eV) of Au in the vicinity of the Fermi energy. The majority-spin band structures are on the left and the minority-spin band structures are on the right. The Fermi level is set to zero. Full lines denote occupied states while dashed lines show empty levels. Note that the 6s level of Au crosses the graphene band structure in the vicinity of the Dirac point but no transfer doping occurs.

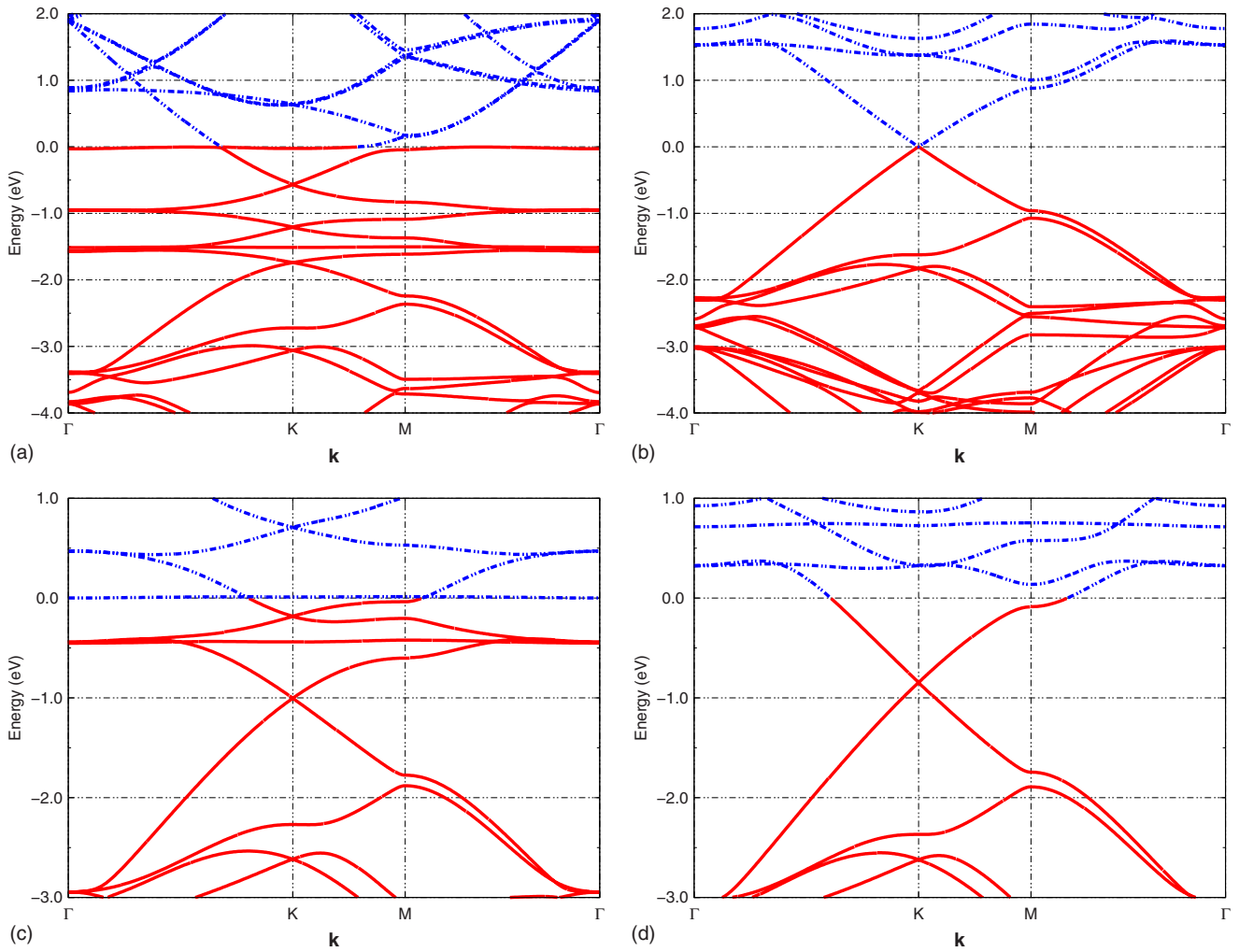


FIG. 9. (Color online) Spin-polarized band structures (eV) of Cr, [(a) and (b)] and Ti [(c) and (d)] in the vicinity of the Fermi energy. The majority-spin band structures are on the left and the minority-spin band structures are on the right. The Fermi level is set to zero. Full lines denote occupied states while dashed lines show empty levels. Note that bands around the Dirac point unoccupied for pristine graphene, are now occupied showing doping behavior.

allows charge transfer to graphene. This might be explained as a consequence of an upward shift of the $6s$ Au level caused by toluene. The band structure is dispersionless near gamma and hybridizes with the π^* graphene bands when they cross near the K point.

Figure 12 shows the wave functions at the levels marked A, B, C, and D in Fig. 11. The wave function of the unoccupied level at Γ , marked A in Fig. 11, is shown in Fig. 12(a)

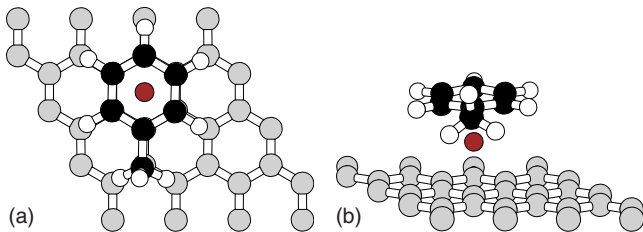


FIG. 10. (Color online) (a) Side and (b) top view of the minimum energy configuration of Ti intercalated with an overlayer of toluene and the graphene surface.

and is clearly localized on Au. However, at the K point, Figs. 12(c) and 12(d) show that the wave function of the occupied levels C and D are delocalized over the graphene surface. Figure 12(d) shows that the unoccupied level at the K point, marked B in Fig. 11 is localized on the Au atom and indicates electron transfer from the $6s$ -Au level to graphene but only when toluene is present.

TABLE III. First column shows the energy required to break the toluene-metal bond while the second shows the energy required to break the graphene-metal bond.

Metals	Toluene (eV)	Graphene (eV)
K	1.06	1.99
Cr	1.95	2.02
Ti	3.08	2.45
Au	0.85	0.80

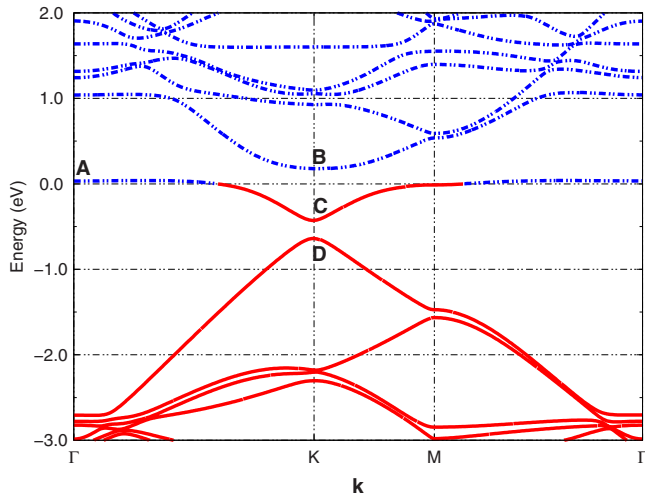


FIG. 11. (Color online) Band structure (eV) of Au intercalated between an overlayer of toluene and the graphene surface in the vicinity of the Fermi energy. Full lines denote occupied states while dashed lines show empty levels. The Fermi level is placed at zero. Note that states near C which were unoccupied for graphene alone are now occupied showing charge transfer has occurred.

The unexpected effect of toluene in enabling electron doping by Au is related to the finding that without toluene, the $6s$ -Au level lies just below the Dirac point but is pushed above when toluene is present. No significant changes in the doping behavior of Ti, Cr, and K atoms were found and this is because the metallic Fermi level is well above that of graphene.

D. Au intercalated into a graphene bilayer

The change in the electronic properties of Au on graphene when an overlayer of toluene is present is probably the result of a confinement of the $6s$ -Au orbital by the layers which has the effect of pushing upward the $6s$ level as for a quantum particle in a box. If this were the case, we would expect that

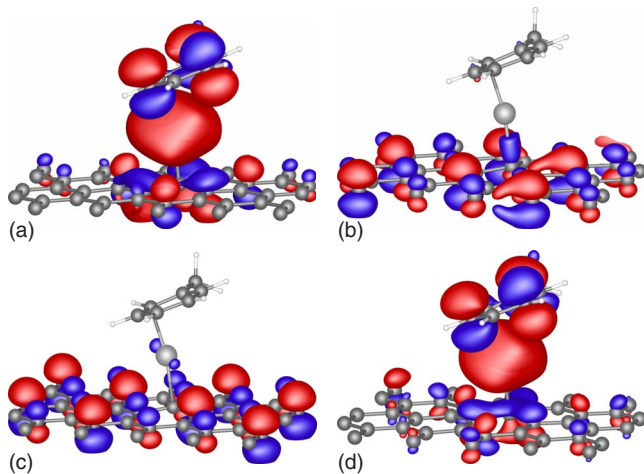


FIG. 12. (Color online) Plot of the real parts of the wave functions for toluene-graphene at the levels marked (a) A, (b) B, (c) C, and (d) D, in Fig. 11.

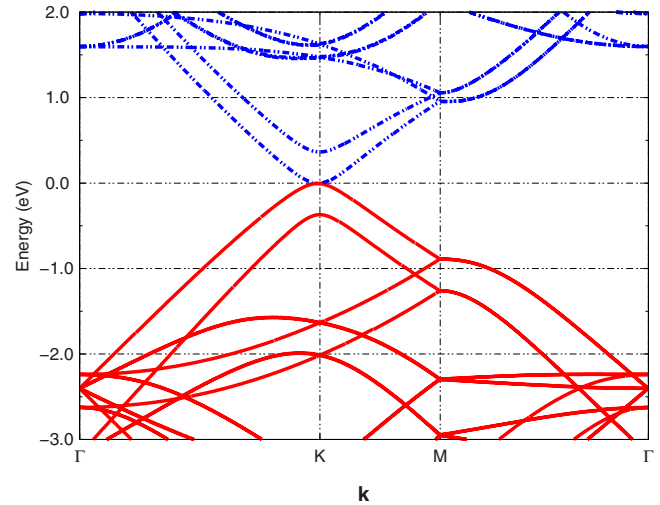


FIG. 13. (Color online) Plot of the electronic band structure of a graphene AB -stacked bilayer along high-symmetry directions. The Fermi level is set to zero. The filled levels are represented by full red lines whereas the empty states are represented by dashed blue lines.

replacing toluene by a second graphene layer would also lead to Au doping.

To investigate this, we used a $4 \times 4 \times 1$ AB -stacked graphene bilayer. Upon relaxation, we found an interlayer separation of 3.3 \AA in good agreement with the interlayer separation in graphite (3.35 \AA).²³ Again there is no net magnetic moment.

The calculated band structure near the Fermi level of an AB -stacked graphene bilayer is shown in Fig. 13. As for single-layer graphene, the highest occupied and lowest empty bands touch at the point K but the linear dispersion is lost. A single Au atom was placed between the graphene layers (Fig. 14). Upon relaxation, the Au atom occupied a site nearly midway between the two graphene layers and 2.14 \AA directly above a carbon atom in the lower layer and directly below the middle of the hexagon of the top layer. The separation between the graphene layers increased to approximately 4.5 \AA . The graphene sheets do not appear to appreciably distort.

The electronic band structure of the Au atom intercalated between the two graphene layers is shown in Fig. 15. The Fermi level is now shifted to lie above the Dirac point. The

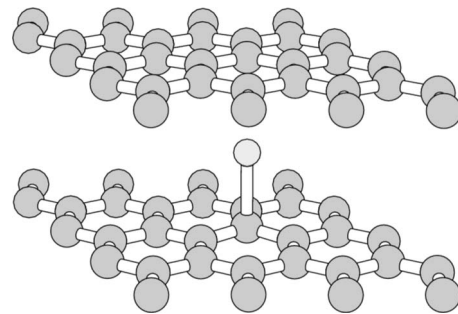


FIG. 14. Equilibrium structure of a Au atom inserted between a graphene bilayer.

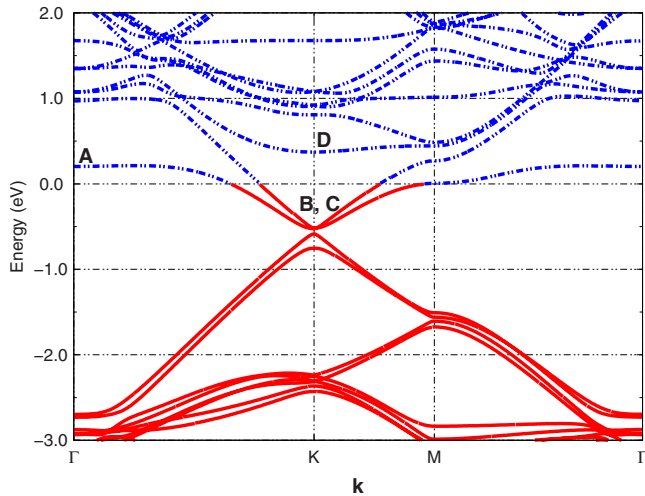


FIG. 15. (Color online) Electronic band structure (eV) for a Au atom intercalated in bilayer graphene in the vicinity of the Fermi energy. Full lines denote occupied states while dashed lines show empty levels. The Fermi level is placed at zero. Note the band marked B which is unoccupied in bilayer graphene is now partially occupied showing doping has occurred.

flat level far from the K point, marked as A Fig. 15, is localized on the Au atom [Fig. 16(a)]. When the $6s$ levels crosses the π^* bands of graphene they hybridize. Charge is transferred to the graphene surface making the graphene n doped. Figures 16(b) and 16(c) shows the wave functions at B and C, Fig. 15, are delocalized over graphene and these levels are now occupied, and unlike the case when the second graphene sheet was absent. The wave function of the empty level marked D (Fig. 15) is shown in Fig. 16(d), and is localized on Au. Thus the effect of a second graphene layer is similar to the effect of toluene and reinforces the view that this is due to a compression of the Au $6s$ -wave function with a consequent upward shift of the $6s$ level.

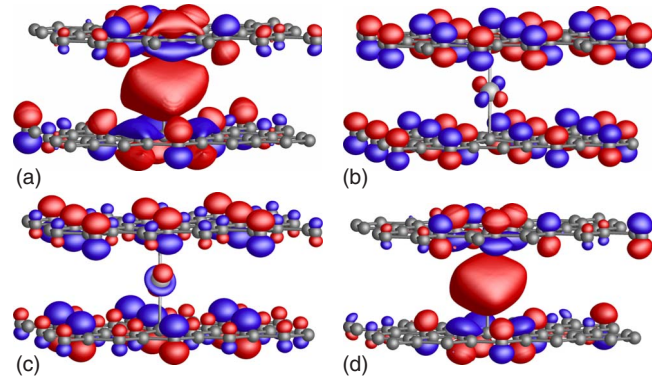


FIG. 16. (Color online) Plot of the real parts of the wave function of Au intercalated into a graphene layer at the levels marked (a) A, (b) B, (c) D, and (d) D in Fig. 15.

IV. CONCLUSIONS

The effect of the adsorption of single metallic atoms on the electronic structure of graphene was studied using spin-polarized density-functional theory in the local-density approximation. K, Ti, and Cr atoms were found to act as n -type dopants in agreement with experiment.^{9,10} Au seemed to be a marginal case with only limited or zero doping. A toluene molecule leaves the electronic structure of graphene unaffected. However, Au intercalated between a graphene sheet and a toluene layer, leads to n doping of graphene. The same effect is found when a Au atom is placed between a graphene bilayer. We suppose the effect comes from a compression of the $6s$ Au wave function with an upward shift of the $6s$ level. An important conclusion is that the properties of adsorbates intercalated between graphene layers, or in contact with hydrocarbon layers, can be different from single-layer graphene. The change in doping character suggests that the Au adsorbed on graphene might be a useful sensor for toluene and other hydrocarbon species.

*pinto@excc.ex.ac.uk

¹K. S. Novoselov, A. K. Geim, S. V. Morozov, D. Jiang, M. I. Katsnelson, I. V. Grigorieva, S. V. Dubonos, and A. A. Firsov, *Nature (London)* **438**, 197 (2005).

²A. H. Castro Neto, F. Guinea, N. M. R. Peres, K. S. Novoselov, and A. K. Geim, *Rev. Mod. Phys.* **81**, 109 (2009).

³K. Ariga, *J. Nanosci. Nanotechnol.* **9**, 1 (2009).

⁴B. Uchoa, C. Y. Lin, and A. H. Castro Neto, *Phys. Rev. B* **77**, 035420 (2008).

⁵K. T. Chan, J. B. Neaton, and M. L. Cohen, *Phys. Rev. B* **77**, 235430 (2008).

⁶Y. Mao, J. Yuan, and J. Zhong, *J. Phys.: Condens. Matter* **20**, 115209 (2008).

⁷H. Sevinçli, M. Topsakal, E. Durgun, and S. Ciraci, *Phys. Rev. B* **77**, 195434 (2008).

⁸H. Rydberg, M. Dion, N. Jacobson, E. Schroder, P. Hyldgaard, S. I. Simak, D. C. Langreth, and B. I. Lundqvist, *Phys. Rev. Lett.* **91**, 126402 (2003).

⁹K. Pi, K. McCreary, W. Bao, W. Han, Y. Chiang, Y. Li, S. Tsai, C. Lau, and R. Kawakami, *Phys. Rev. B* **80**, 075406 (2009).

¹⁰J. H. Chen, C. Jang, S. Adam, M. S. Fuhrer, and E. D. Williams, *Nat. Phys.* **4**, 377 (2008).

¹¹F. Schedin, A. Geim, S. Morozov, E. Hill, P. Blake, M. Katsnelson, and K. Novoselov, *Nature Mater.* **6**, 652 (2007).

¹²T. Wehling, K. Novoselov, S. Morozov, E. Vdovin, M. Katsnelson, A. Geim, and A. Lichtenstein, *Nano Lett.* **8**, 173 (2008).

¹³W. Chen, S. Chen, D. Qi, X. Gao, and A. Wee, *J. Am. Chem. Soc.* **129**, 10418 (2007).

¹⁴H. Pinto, R. Jones, J. P. Goss, and P. R. Briddon, *J. Phys.: Condens. Matter* **21**, 402001 (2009).

¹⁵R. Jones and P. R. Briddon, *Semicond. Semimetals* **51**, 287 (1998).

¹⁶M. J. Rayson and P. R. Briddon, *Comput. Phys. Commun.* **178**, 128 (2008).

¹⁷C. Hartwigsen, S. Goedecker, and J. Hutter, *Phys. Rev. B* **58**, 3641 (1998).

- ¹⁸J. P. Goss, M. J. Shaw, and P. R. Briddon, *Top. Appl. Phys.* **104**, 69 (2006).
- ¹⁹H. J. Monkhorst and J. D. Pack, *Phys. Rev. B* **13**, 5188 (1976).
- ²⁰D. Andre, R. Fourme, J. Bruneaux-Pouille, and L. Bosio, *J. Mol. Struct.* **81**, 253 (1982).
- ²¹R. Zacharia, H. Ulbricht, and T. Hertel, *Phys. Rev. B* **69**, 155406 (2004).
- ²²P. A. Khomyakov, G. Giovannetti, P. C. Rusu, G. Brocks, J. van den Brink, and P. J. Kelly, *Phys. Rev. B* **79**, 195425 (2009).
- ²³J. C. Slonczewski and P. R. Weiss, *Phys. Rev.* **109** 272 (1958).